Proc. Lunar Planet. Sci. Conf. 10th (1979), p. 1897–1916.
Printed in the United States of America

A special class of planetary collisions: Theory and evidence

William K. Hartmann

Planetary Science Institute, Tucson, Arizona 85719

Abstract—Collisions between comparable-sized planetary bodies are a special class of collisions, rarer than other collisions, but producing interesting products, such as unfractured dumbbell-shaped contact binaries, partly brecciated elongated bodies, totally breciated spheroidal bodies, and perhaps co-orbiting binary pairs or swarms. Qualitative and rough quantitative theories are presented to indicate collision outcomes. Contact binaries or fractured elongated bodies as large as tens or hundreds of kilometers across can be produced—larger than hitherto considered. Lengths about 20 to 200 km are most probable for igneous or ordinary chondritic elongated objects formed by collision, but other lengths could result from tidal evolution of pairs. Though most elongated asteroids are probably collision fragments, as usually assumed, some may instead be accretionary products. Trojan asteroid 624 Hektor is a candidate. Some polymict, genomict, and monomict brecciated meteorites may be better explained by large-scale fragmentation and immediate gravitational re-assembly of parent bodies than by local-scale processes of cratering on parent-body surfaces.

INTRODUCTION

A great deal of evidence shows that many collisions have occurred among planetary objects as the planets formed, and that these explain many features of meteorites (Herndon and Wilkening, 1978) and of the present day planetary system (Safronov, 1972; Hartmann and Davis, 1975; Wetherill, 1976; Hartmann, 1968, 1977; Greenberg *et al.*, 1978). Craters on all the planets, certain orbital characteristics, polymict brecciation of meteorites, and size distributions of asteroids are among the properties explained by such collisions. The experimental and theoretical mechanical modelling of these collisions is just in its infancy. Collisional velocities of asteroids (long considered to be mostly fragments from such collisions) and velocities of bodies hitting the moon have influenced the conceptual framework for treating such collisions. The former velocities are of the order 5 km/sec and the latter, about 10–20 km/sec, and most published treatments of planetesimal collisions have thus treated the velocity regime of several kilometers per second (Gault *et al.*, 1963; Fujiwara *et al.*, 1977). Furthermore, because of the size distributions involved, the vast majority of collisions in the solar system today and probably during the formative states involved pairs of bodies with mass ratios much different from unity. Although few general conceptual frameworks have been presented for classifying all of the possible collisional outcomes, a survey of the literature indicates that most workers treat the outcomes as falling

in the categories of (a) cratering (small bodies excavating debris on a large body, high velocity; Gault *et al.*, 1963), or (b) catastrophic fragmentation of both bodies with products usually being dispersed (Fujiwara *et al.*, 1977). Hartmann (1977) studied (c) the low-velocity regime of rebound of one body off the other with no fracturing or fragmentation, and emphasized that in the early solar system, velocities were so low that rebound off the largest bodies would often result in fallback, hence accretion.

Greenberg, Wacker, Hartmann, and Chapman (1978) synthesized these results into a numerical simulation of collisional evolution that allowed for regimes of rebound without cratering, rebound with cratering of both bodies, shattering of the smaller body, and shattering of both bodies. When shattering occurred, this program used certain velocity distributions and computed whether mass escaped or all re-assembled due to gravity. It then inserted the post-collision mass(es) into appropriate mass bins which were used to keep track of the evolving mass distribution. It did not, however, describe the specific nature of collision products so produced, nor did it further distinguish the future histories of homogeneous large bodies grown of accumulation of small bodies, from the histories of heterogeneous, fractured, large bodies resulting from collision of pairs of large, comparable-sized bodies. The present paper calls attention to the special properties of the latter type of collision, which may produce unique or highly interesting objects.

Recent studies of Trojan asteroid 624 Hektor by Hartmann and Cruikshank (1978), enlarging on earlier studies of the same asteroid by Dunlap and Gehrels (1969) and Cook (1971), suggested that Hektor is a 300-km-long dumbbell-shaped compound planetesimal formed by a relatively low-speed collision of two 150-km-scale spheroidal asteroids, with incomplete fragmentation and partial coalescence. Such a low-speed collision might occur directly during circulation around the Lagrangian points in Jupiter's orbit, where Trojan asteroids are located, or might result from inward tidal evolution of a co-orbiting pair. Hektor is the largest Trojan and roughly twice the size of the next largest Trojans, which are roughly spheroidal, not elongated, according to their lightcurves. Hektor thus seems unlikely to be merely an irregular-shaped fragment. Obviously, a compound planetesimal would be highly unusual compared to the conventional concept of planetary bodies, and would provide an interesting target for close-range exploration. Hence, the Hektor model has prompted the present further investigation of such collisions.

Little attention has been paid to the specific class of collisions when two bodies are of comparable size. This type of collisions is currently rare, compared to the other collisions. Due to the shape of the size distribution of small bodies, collisions with small bodies hitting much larger bodies are by far the most common. Nonetheless, some collisions of comparable size bodies have surely occurred in the infinitude of planetary encounters in the solar system's history. Such collisions may have been more representative in the past, since calculations indicate that gravitational collapse of the dust component in the original solar nebula produced

not the current size distribution, but a group of bodies of a certain characteristic size, a point to which we will return later.

We will now develop a general framework for considering collisions of comparable-size bodies. For simplicity, we will assume here that the two bodies under consideration are of equal size. A later section considers cases of nearly equal size.

QUALITATIVE DESCRIPTION OF PHENOMENA

To begin with a qualitative discussion, the ordinate on Fig. 1 is the initial energy density (energy/volume, infinite separation), a quantity determined solely by the initial approach velocity (indicated at right). The abcissa on Fig. 1 is the infall energy density, that is, the energy density derived by letting the two bodies fall together from infinity; this quantity is determined solely by the radius of each of the two bodies as shown at the top, assuming uniform density. For a given composition, hence, mechanical properties, these two parameters should suffice to

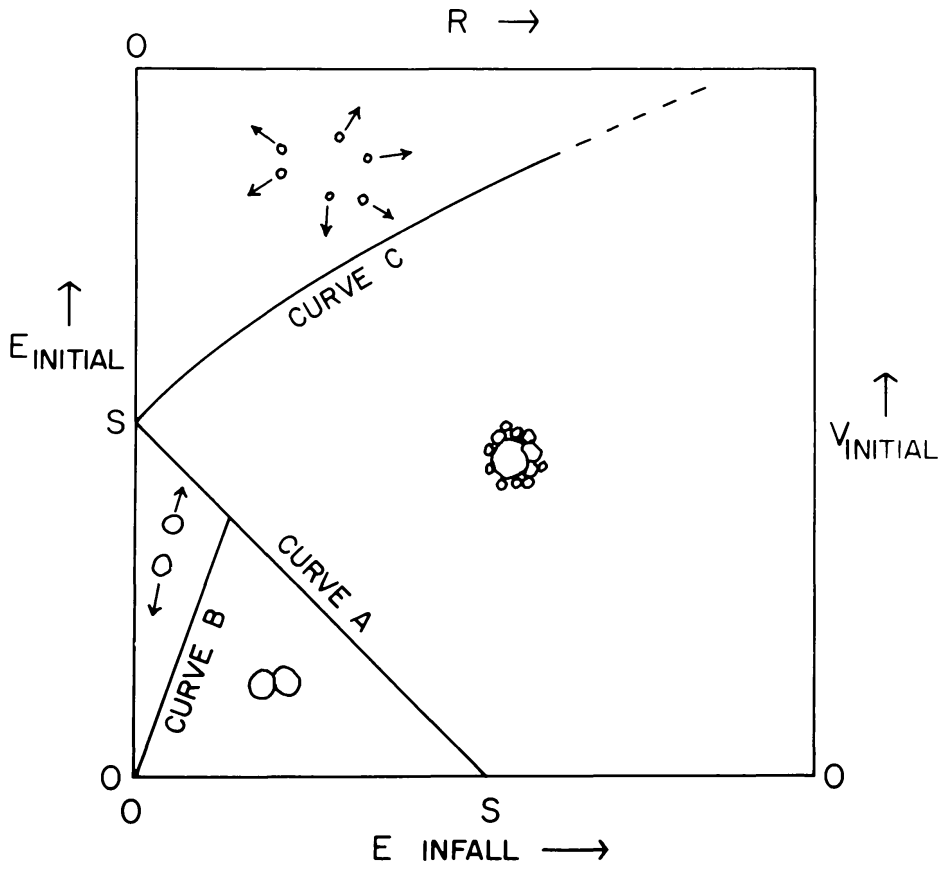

Fig. 1. Qualitative diagram of the collision regimes for equal-sized bodies, defining curves A–C discussed in the text. Collision outcomes are determined by initial approach velocities, size of bodies, and bodies' mechanical properties. Cartoons show four outcome regimes divided by the curves.

determine the outcome of the head-on collision. (Further variations, not considered here, could result from glancing collisions). We thus define:

E_{impact} = kinetic energy/volume at impact;

$E_{initial}$ = relative kinetic energy/volume at very large separation distances; (1)

E_{infall} = kinetic energy/volume generated when two equal-sized bodies fall together under their own gravity from infinite separation.

The phase space in Fig. 1 is divided by three important boundary curves. These boundary curves are actually defined by parameters which have a range of transitional values, some of which are uncertain. However, to clarify the nature of these curves, we assume for the moment that they can be defined by certain mean effective parameters.

A certain curve, A, divides a region where the total energy density is insufficient to fragment catastrophically the body, from a region where it is sufficient. This curve, A, is given by

$$f(E_{impact}) = S = f(E_{initial} + E_{infall}) \quad (2)$$

where S = energy/volume required to fragment the body catastrophically, and f = the fraction of energy available for fracturing material $\simeq 0.2$ (O'Keefe and Ahrens, 1978). Catastrophic impact was defined (Greenberg *et al.*, 1978) as a fragmentation in which the largest fragment equalled half the original mass. Fujiwara *et al.* (1977) and Hartmann (1978) measured velocities (hence energy densities) required to fragment colliding bodies of different materials, and Greenberg and Hartmann (1977) formulated a conception of impact strength, S, from these measures, so that some relevant quantative data are available.*

Curve B divides the rebound regime from the fall back regime in sub-fragmentation space. This curve derives from experiments of Hartmann (1978), who showed that for two bodies with negligibly thin regolith layers, low speed impacts resulted in non-fracturing rebound. The rebound velocity was 85% of the impact velocity for smooth basalt spheres, but typically half the impact velocity or less for irregular, natural igneous rocks (partly due to the loss of energy into vibration and spin). The rebound velocity drops dramatically when regolith layers have thickness comparable to projectile diameters. Curve B is drafted for the assumption that rebound occurs at half the impact velocity, as might be true for clean, rocky bodies. In this case, for two equal size bodies, we have

$$E_{rebound} = \rho V_{rebound}^2 = \rho(V_{impact}/2) = E_{impact}/4. \quad (3)$$

---

* *NOTE ADDED IN PROOF:* S dependence on mass and velocity, if any, is highly uncertain The author is undertaking experiments (June 1979) at the newly-opened Ames Vertical Gun Facilit to investigate this.

Since the infall energy is equal to the energy for the two bodies to escape from each other, curve B is defined by the condition

$$E_{rebound} = E_{infall} \equiv E_{impact} - E_{initial}. \quad (4)$$

Thus,

$$E_{initial} = E_{impact} - E_{infall} = 4E_{rebound} - E_{infall} = 4E_{infall} - E_{infall} = 3E_{infall}.$$

In the region of fragmentation beyond Curve A, another curve, C, separates a regime where the fragments (or a fraction thereof) will disperse to infinity, from a regime where they will fall back together by their own gravity. This curve, C, is given by the condition that the total initial energy equals energy sufficient to fragment the body plus energy sufficient to disperse a certain fraction of the fragments to infinity. In analogy to catastrophic fragmentation, let us define catastrophic dispersal as a condition when half the fragments are dispersed to infinity, and the remaining half fall together again to make a brecciated body. Furthermore, let us define dispersive fragmentation as a condition when all fragments disperse to infinity. This is undoubtedly idealized, since it is difficult to prevent certain pairs of fragments from re-aggregating even as they disperse from the impact site, while other fragments may end up in orbit around each other, dependent on the chaotic dispersal of large fragments, dust, and vapor from the collision. For our idealized curve, C, we represent dispersive fragmentation by

$$kE_{impact} = S + E_{total\ dispersal}, \quad (5)$$

where

k = fraction of E_{impact} available for fracturing and ejecta kinetic energy
= 1 − fraction of E_{impact} used in plastic work and heating,

where

$E_{total\ dispersal}$ = energy/volume required to disperse all materials from post-impact configuration to infinity
$\simeq E_{infall}$.

Since the impact energy density is the initial energy density plus infall energy density, we then have

$$kE_{initial} + kE_{infall} = S + E_{total\ dispersal}. \quad (6)$$

In Fig. 1, curve C is schematically drafted with an arbitrary curvature.

Qualitative consideration of the simple curves divide the number of possible outcomes into four possibilities, shown by the cartoons in Fig. 1. In the lowest triangular box, the initial energy and infall energy combined are insufficient to allow the particles either to fragment or rebound so that they fall together intact and form a dumbbell-shaped figure. In the triangle above Curve B, the energy is now sufficient to allow the particles to rebound from each other to infinity, but insufficient to fragment them. In the region to the right of Curve A, the combi-

nation of initial and infall energies is sufficient to catastrophically fracture the bodies, but insufficient to allow the fragments to rebound, so that a granular body reforms from the various fragments. Such a granular body might eventually weld into either a monomict or polymict breccia, depending on the degree of mixing of fragments from different parts of the original bodies. Interestingly, this means that polymict breccia meteorites do not *necessarily* involve fragments from different parent bodies, since some parent bodies almost certainly had heterogeneous interiors. Above Curve C, the energy is so great that the fragments disperse. Curve C meets Curve A at the left margin for $E_{initial} = S$ because this is the transition from non-fragmenting to fragmenting collisions for zero-radius particles, for which no energy is required beyond fracturing to disperse the bodies ($E_{total\ dispersal}$ in Equation (6) is 0, in this case).

A better understanding of the phenomenon involved can be gained by considering the transitions that occur near each of these three bounding curves. Figure 2 attempts to describe the transitions qualitatively by cartoons. In Cartoon A, two very small bodies fall together at such low speeds that there is not enough

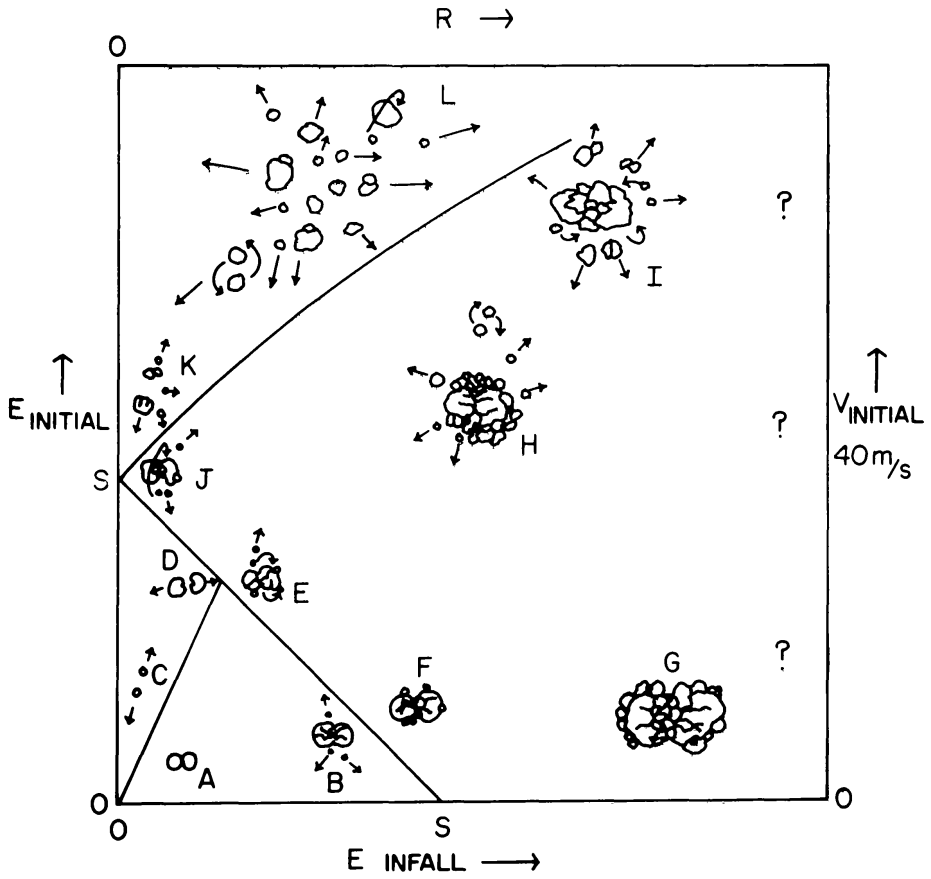

Fig. 2. Same as 1, but with cartoons showing that the collisional outcome regimes grade through transitions into one another. Sketches A–L show various outcomes discussed in text. Question marks at right are a reminder that while small-scale outcomes have been verified in the lab, scaling to large dimensions is very uncertain.

energy for any fracturing nor to bounce the particles apart. In B, the impact has occurred fast enough for some fracturing to occur, but not catastrophic fracturing. The resulting body is partly fractured. In C, the bodies are so small that there is not enough gravity to hold them together and since there is not enough velocity to fracture them, they simply bounce apart undamaged. In D, they also rebound, but there is enough energy to cause some minor chipping. In E and F, we are across the line of catastrophic fragmentation, but much of the available energy goes into simply fracturing the body so that the pieces come to rest almost *in situ,* and there is very little energy to redistribute them. In G, the bodies are large, but the initial velocity is still so low that, while much fracturing occurs, there is little excess energy to overcome gravity and throw off or redistribute fragments. In H and I, there is considerable excess energy, and we are well beyond catastrophic fragmentation. Many pieces are very small, and are ejected at high speed. Others are mixed and fall back together; many fragments are ejected entirely. Some ejected pieces may be partially reconsolidated bodies or even co-orbiting bodies. Cases J and K are just in the transition region between rebound, catastrophic fragmentation, and total dispersal. In J, there is just enough energy to substantially fragment the body, but not enough extra to totally disperse the material. In K, the bodies disperse, probably in the form of two major pieces which represent the rebounding course. In L, there is so much excess energy that the body is completely shattered and pieces are widely dispersed, though some pieces may interact causing polymict breccias or co-orbiting pairs.

QUANTITATIVE DESCRIPTION: BASALT-LIKE PLANETESIMALS

A quantitative treatment of the same diagram can be derived by fitting available experimental data into the equations. Since velocities and sizes are more useful conceptually then $E_{initial}$ and E_{infall}, we will derive the curves in those terms. Let

M = mass of each body
V_I = initial approach velocity at infinite separation (relative orbital velocity)
R = radius of each body
ρ = density of each body
S = impact strength (ergs/cm^3).

The best data are available for basalts and other igneous rocks. We will begin by assuming basalt as the nominal material with density 3 g/cm^3. A following section will derive the same curves for a weaker, more granular material.

Then to derive Curve A, we have

$$E_{initial} = 1/2 \frac{MV_I^2}{vol} + 1/2 \frac{MV_I^2}{vol} = \rho V_I^2 \tag{7}$$

$$E_{infall} = \frac{GMM}{2R(\text{total volume})} = \frac{GM\rho}{4R} = \frac{\pi G \rho^2 R^2}{3}. \tag{8}$$

Hartmann (1978) found that basalt spheres and natural igneous rocks shattered catastrophically upon striking a much larger flat rock target at 4×10^3 cm/sec, giving S_{basalt} (assuming half the kinetic energy goes into target and projectile each):

$$S_{basalt} = 1/2 \cdot 1/2 \frac{MV_{impact}^2}{vol} = 4(10^6)\rho. \quad (9)$$

A similar result comes from measures on basalt at V_{impact} = 1–3 km/sec (Fugiwara *et al.*, 1977). Thus, equation (2) for Curve A becomes:

$$V_I^2 = 4(10^6) - 2(10^{-7})R^2. \quad (10)$$

Curve B is given by applying equations (7) and (8) to (4):

$$V_I = 9(10^{-4})R. \quad (11)$$

Curve C is derived from equation (6), giving

$$kE_{initial} \simeq S + (1 - k)E_{infall}.$$

For a basaltic body, equations (6)–(9) give

$$V_I^2 = \frac{1.3(10^6)}{k} - \frac{1 - k}{k} 2(10^{-7})R^2. \quad (12)$$

O'Keefe and Ahrens (1977) give data on k. For impacting igneous rocks, they calculate (1 − k), the fraction of energy lost in heating of the meteorite and target, as increasing from 0.4 to 0.6 as V_{impact} increases from 5 to 30 km/sec; and they quote Gault and Heitowit (1963) as deriving experimental values from 0.2 to 0.35 for this fraction at V_{impact} = 6 km/sec. They assert the latter values are underestimates. The rest of the energy they assign to (comminution + plastic work), and (ejecta kinetic energy). If we assume the energy available for (comminution + ejecta KE) = 1/2 (comminution + plastic work) + (ejecta KE), then we derive k = .35 to .25 as V_{impact} increases from 5 to 30 km/sec, and k = .8 to .5 from the Gault and Heitowit experimental data. The difference is primarily due to the high kE estimated by Gault and Heitowit, which O'Keefe and Ahrens assert is overestimated. At lower, subsonic impact speeds, we can estimate that k is higher, and less energy goes into heating. We therefore assume in applying equation (13) that k decreases roughly linearly from 0.8 for speeds below 0.1 km/sec to k = 0.3 for speeds about 10 km/sec. As emphasized by O'Keefe and Ahrens (1977), better data on the energy partitioning parameter k are needed in order to understand collision results.

Figure 3 shows the quantitative results derived for collisions of equal-sized basalt-like bodies. The belt asteroids are in the regime of catastrophic or total disruption during collisions involving their mean approach velocities of about 5 km/sec. Depending on the distribution of asteroid approach velocities around

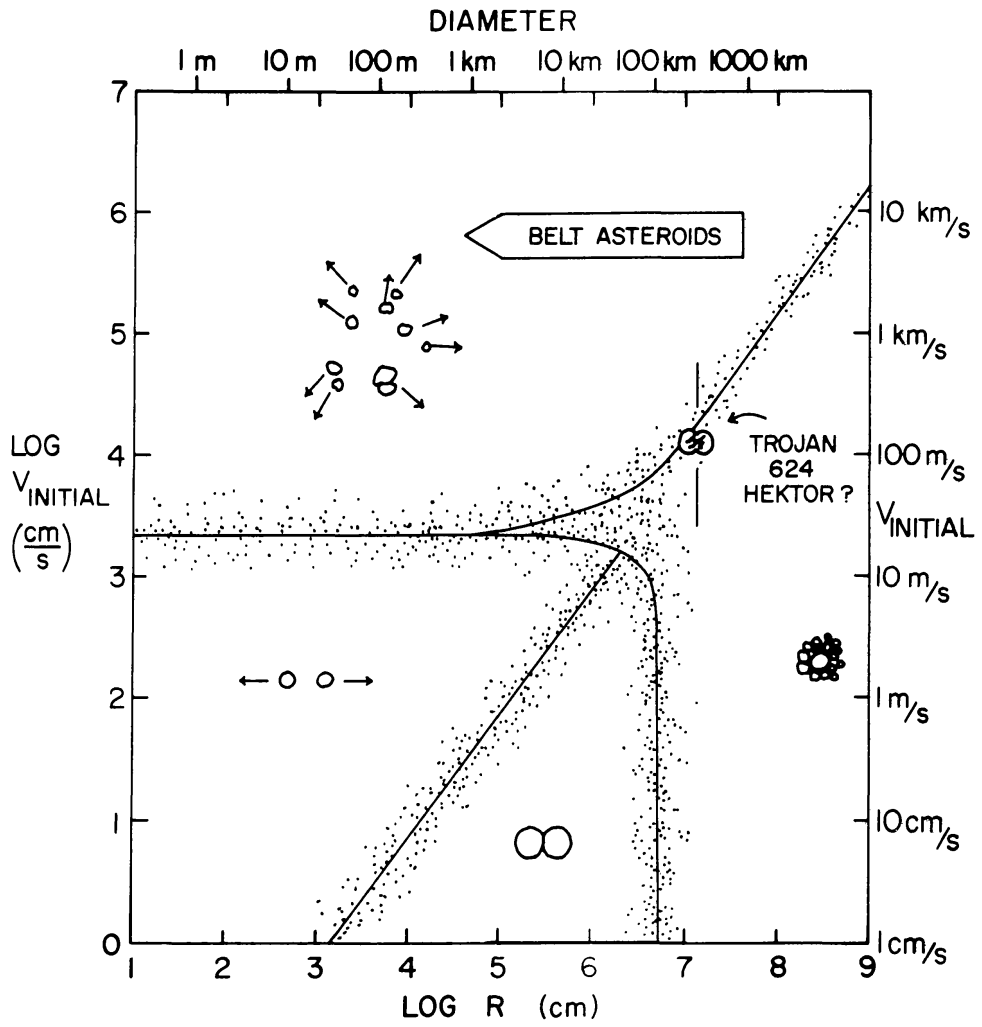

Fig. 3. Quantitative version of Fig. 1, based on equations in text, and using log scales instead of linear scales, thus altering shapes of curves A–C. Stippling indicates transition zones. Five main types of outcomes are illustrated by cartoons: the four major regimes and the important transition between unfractured contact binaries and reassembled brecciated spheroids. This transition produces fractured elongated objects probably extending up to the size of Trojan asteroid 624 Hektor. A collision velocity below about 10^2 m/s would apparently be needed to produce Hektor, though more probable velocities in the Trojan cloud would be higher, as indicated by vertical line. This diagram calculated for material with properties resembling basalt or other igneous rocks.

this mean, low-velocity collisions between pairs with similar orbital elements may occasionally result in contact binary pairs or elongated fractured bodies near the transition zone along the vertical part of curve A. Based on the upper tip of the elongated body and transition regimes in Fig. 3, the most likely diameters for such bodies, assuming basalt-like strengths, would be around 10 to 300 km. Consistent with Hartmann and Cruikshank (1978) the elongated Trojan asteroid 624 Hektor as marked in Fig. 3, may be such an object, as discussed further below.

QUANTITATIVE DESCRIPTION: REGOLITH-COVERED CARBONACEOUS-CHONDRITE-LIKE PLANETESIMALS

It is interesting to contrast the preceding with results for much weaker bodies. The present asteroids, and many meteorite parent bodies of the past may have mechanically resembled igneous rocks after an early period of melting-heating, or metamorphism. However, the earliest planetesimals, perhaps formed by gravitational collapse or collisional accretion of dust would not have these igneous properties. Crumbly carbonaceous chondrites resembling hard dry soil are known; such primitive material may be consolidated largely by cementing by residues of evaporites, rather than by solidification of a molten mass. Primitive aggregates are also likely to have a granular surface regolith of impact-derived material, which markedly changes their low-speed collision properties.

We now rederive curves A, B, and C for weak bodies (henceforth designated PP for primitive planetesimal) with density $\rho = 2$ and loose surface layers, or best as is possible from available data. Hartmann (1977) found catastrophic fragmentation for dirt clods at $V_{impact} = 2$ m/s, giving in place of equation (9):

$$S_{PP} \simeq 1(10^4)\rho. \tag{9A}$$

Curve A for our PP body is thus given by a modification of equation (10):

$$V_I^2 = 10^4 - 1.4(10^{-7})R^2. \tag{10A}$$

Hartmann (1977) also found that for impacts into granular targets in vacuum, elastic properties of rocks were effectively destroyed by a thin layer of regolith powder (mechanical properties resembling lunar regolith) because of energy dissipation in moving the regolith grains. For example, a regolith layer ½ as deep as an incoming particle's diameter, overlying coherent smooth rock, reduced the rebound velocity to about 0.03 × its impact velocity. Assuming this value as representative of a planetesimal (instead of 0.5 used in equation 3), equation (3) becomes

$$E_{rebound} = \rho V_{rebound}^2 = \rho(0.03 V_{impact})^2 = 9(10^{-4})E_{impact} \tag{3A}$$

and equation (11) becomes modified to give curve B:

$$V_I = 1.6(10^{-4})R^2. \tag{11A}$$

Curve C for our PP body is given by equations (6), (7), (8), and (9A) as a modification of equation (12):

$$V_I^2 = \frac{10^4}{k} + \frac{(1-k)}{k}1.4(10^{-7})R^2. \tag{12A}$$

The value of k is less certain than before, in the absence of published values of the partition of energy in such material. However, Gault's and other's experiments suggest that less energy goes into ejecta than in the basalt case (see review of relevant data by Greenberg *et al.*, 1978, p. 5, and we assume k decreases

roughly linearly from 0.5 for speeds below 0.1 km/sec to 0.1 for speeds about 10 km/sec.

Figure 4 shows the equivalent of Fig. 3, but for the postulated PP, or carbonaceous chondrite-like bodies with granular regoliths of appreciable depth (0.1 to 0.3 radii?). As expected, the region for total fragmentation is expanded. However, it is easier for the weak, regolith-covered bodies to accrete because they are very inelastic, and curve B thus shifts to the left. At approach velocities of 10 cm/sec, PP bodies of diameter about 15 m to 411 km can form contact binary pairs, or transitional elongated, fractured bodies, contrasted with a diameter range of perhaps 10 to 300 km for basaltic bodies.

UNCERTAINTIES AND EVOLUTIONARY TRACKS

Figures 3 and 4 include stippled bands that roughly illustrate the uncertainties in the derivations, and the regions of transitions from one distinct outcome to another. Among the uncertainties are the value of k that should be used in curve C. A shift in k from 0.9 to 0.1 increases V by about 30 times for a fixed R value.

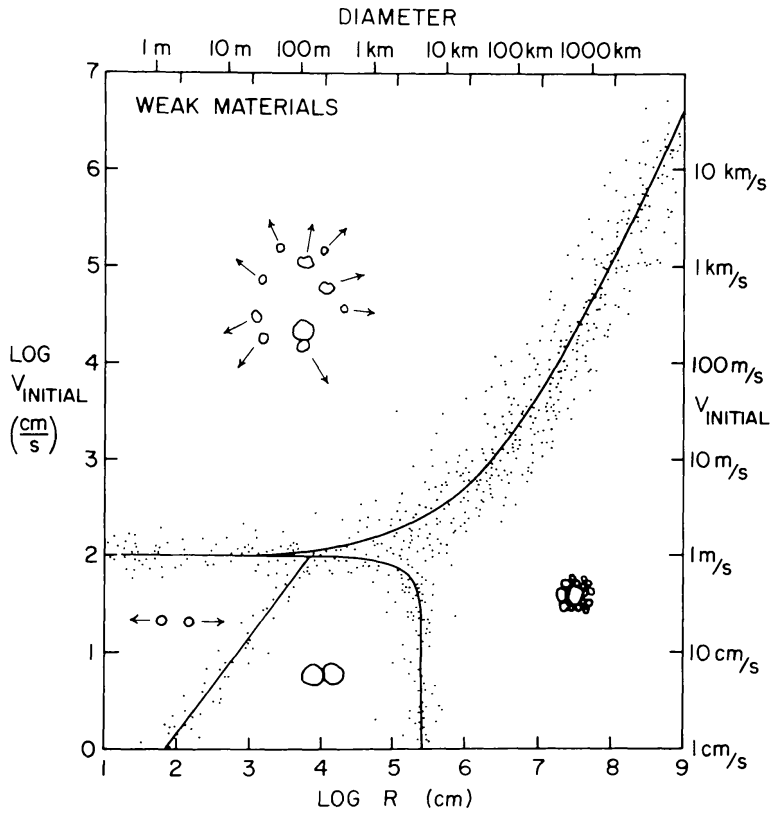

Fig. 4. Same as Fig. 3, but calculated for bodies with material properties of weakly consolidated dry soils, probably resembling weak carbonaceous chondrites. The fracturing regimes are expanded because of the lower strength, and the contract binary zone is widened because of lower elasticity, reducing the rebound velocities.

Transitions are also broadened by the range of energies corresponding to different degrees of fragmentation on curve A, and the range of rebound velocities caused by different degrees of spin and different material properties in curve B. It is thus very difficult to say how, for example, the elongated dumbbell shape of two unfractured spheres in contact (left of lower curve A) changes into an elongated shape of two partly fractured spheres (right of curve A), and when there is enough energy to disassemble the fragments sufficiently that they reaccumulate in a spheroidal, rather than elongated, body.

An especially important problem is how fragmentation events scale upward with size. The energy densities for fragmentation have been determined empirically in the lab for 1–10 cm-scale bodies. Öpik (1965) has argued that many cratering and fracturing phenomena scale with momentum, not energy, though energy scaling appears to fit lab data over several orders of magnitude in velocity. Furthermore, the mode dissipation of impact energy through the body is important. For example, in small bodies colliding at subsonic speeds, seismic waves carry the energy through the volume of the body before penetration is appreciable. But in large bodies colliding at supersonic speeds, the impact energy is at first concentrated in a quasi-hemispherical volume around the impact point with an energy density for above the impact strength; moments later, the projectiles have interpenetrated to greater depth, consuming a large fraction of the available energy, and the shock wave spreads to much large volume with declining energy densities. For these reasons, the collisions of small and large bodies at various speeds cannot be considered homologous processes. Collisions at lunar and planetary scales, especially, involve unknown quantities, such as variable internal temperature and strength. These scaling problems add unknown uncertainty to the boundaries mapped at either $R \gtrsim 10^5$ cm or $V \gtrsim 10^4$ cm/sec.

Nonetheless, the existing data clearly show that four general outcomes result from collisions of comparable-sized bodies. Small, slow bodies can rebound off each other with no resultant growth. Larger, slow bodies will fall together without serious fracturing and form dumbbell-shaped contact binary pairs. This phenomenon can occur at diameters as large as a few kilometers in weak material and 10^2km or more in basalt-like rock material. Still larger bodies shatter but reassemble in roughly spheroidal granular bodies that may cement into breccias. Faster bodies can disrupt each other entirely and produce only fragments of various sizes, possibly including breccias and pairs.

To these four outcomes, we add a fifth important outcome that lies along the transition zone marking the vertical part of curve A (cases E, F, J in Fig. 2): it is a highly fractured, elongated body where energy is used to fracture the two colliding bodies, but not enough remains to blow them apart and allow reassembly into a sphere. It is the transition between unfractured contact binaries and brecciated spheroids, distinguished by having both intense fracturing and elongated shape.

Figures 5 and 6 replot Figs. 3 and 4 at the same scale without the uncertainty bands, but with two additional features. First, dashed lines are added indicating when the approach velocity $V_{initial}$ equals the escape velocity (V_{esc}) and 1/10 V_{esc}.

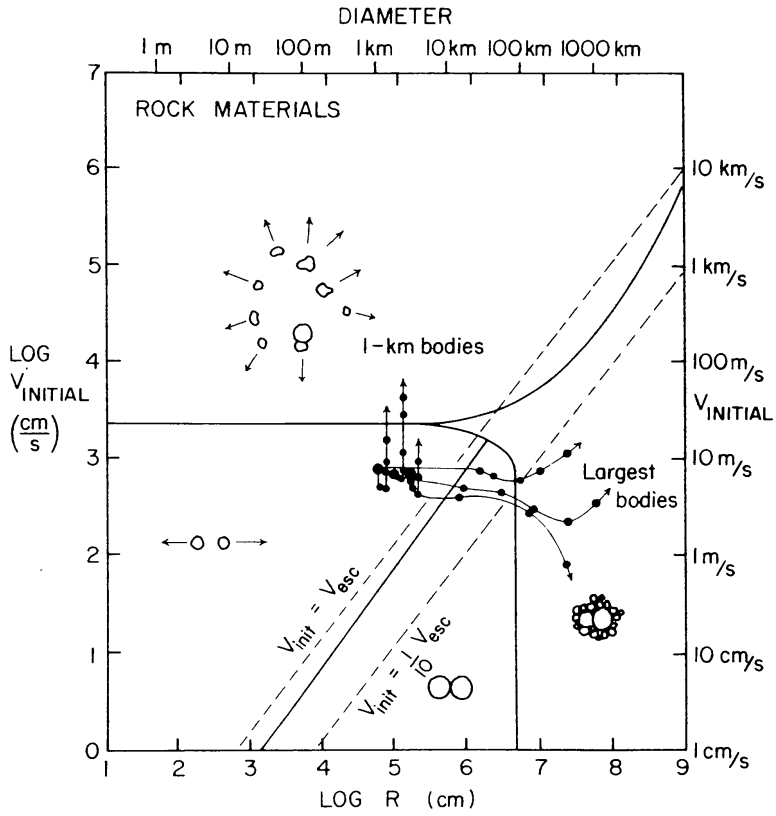

Fig. 5. As Fig. 3, but with addition of dashed curves relating the initial velocity to the escape velocity of the bodies, and evolutionary tracks taken from numerical simulation of planetesimal evolution by Greenberg *et al.* (1978). The upper two tracks are for solid rock planetesimals, well-suited to this diagram. The lower track is for weaker, less elastic planetesimals, departing somewhat from the material assumed in the diagram. The three starting points assumed by Greenberg *et al.*, are shown by heavy black dots; the evolutionary tracks for bodies in the 1-km size bin show how their velocities evolve upward due to gravitational effects of the accreting larger bodies. Tracks to the right show the evolution of the largest bodies. Largest bodies in all cases considered evolved across the contact binary regime into the regime of intensely brecciated spheroids, suggesting that whenever large asteroids collided, they produced re-assembled bodies with brecciated interiors (either before or after possible melting episodes). Note that large asteroids never hit by comparable-sized bodies would have different interiors.

These lines are usefully compared with Safronov's (1972) finding that equilibrium approach velocities in a planetesimal swarm in a toroidal volume at some distance from the sun will tend to evolve toward equilibrium values equal to the escape velocity of the largest bodies in the swarm—a finding modified by Greenberg *et al.* (1978) and Levin (1978) to the statement that in practice, the approach velocities tend to equal escape velocities not of the largest bodies but of somewhat smaller and more numerous bodies. Hence, we can expect actual approach velocities in early swarms to be between the dashed lines or near the lower dashed line, based on model studies (Greenberg, *et al.*, 1978). This shows that interactions between the largest equal-sized early planetesimals, when they occurred, usually resulted in formation of unfractured contact binary pairs; or fractured,

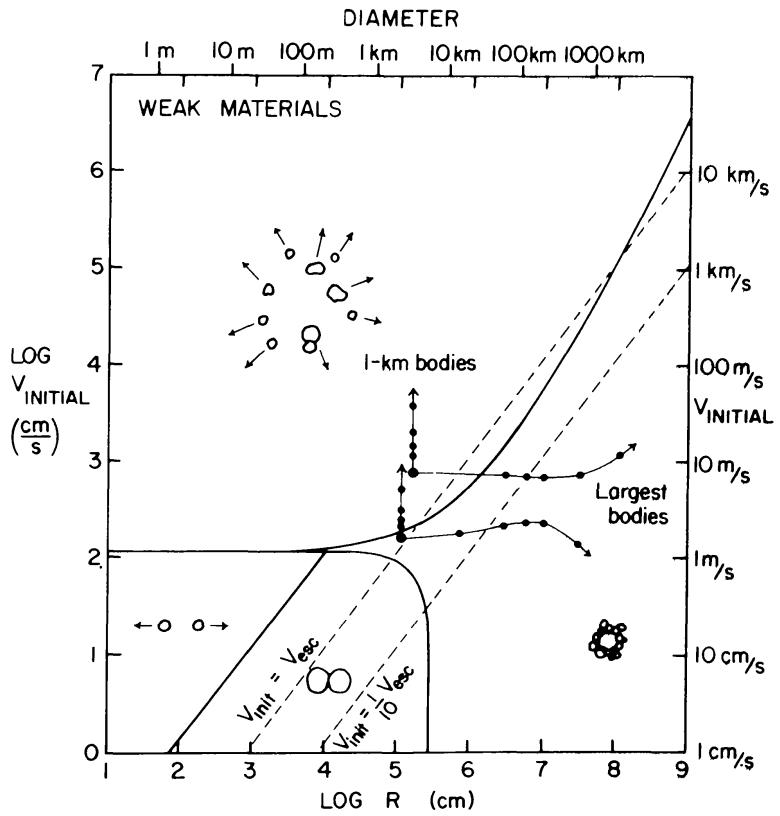

Fig. 6. As Fig. 5, but for weak materials. The lower evolutionary track (Greenberg *et al.*, 1978) is for weak, loosely bonded material very similar to that for which the background diagram was calculated. The upper curve is for somewhat stronger material. As in Fig. 5, the 1-km bodies evolve to high velocities, but the largest bodies evolve into the regime of accreting, brecciated spheroids.

partly-coalesced elongated objects; or fractured, reconsolidated spheroidal bodies.

The second feature added to Figs. 5 and 6 is a group of evolutionary tracks showing paths followed by planetesimals in the numerical simulations by Greenberg *et al.* In some of these simulations, the initial approach velocities were arbitrarily chosen to exceed escape velocities of the 1 km bodies in the initial swarm; these mean velocities usually decreased until a few low-velocity collision produced coalesced larger bodies which began to grow by sweeping up remaining small bodies. The growth led to a pumping up of velocities of remaining small bodies. Therefore, two sets of instructive evolutionary tracks are plotted in Figs. 5 and 6. One set of tracks evolves from the initial points upward along the R = 1 km line; these represent the histories of R = 1 bodies during the planet-accreting process. The second set of tracks evolves to the right toward larger sizes; these represent the largest bodies found in the numerical simulation at each time. The pairs of tracks show dramatically that while the *small* "remainder bodies" get pumped up in velocity into the regime where comparable-sized bodies collide in total fragmentation, the *largest* bodies evolve into the regime where equal-sized

bodies produce either contact binaries (all three tracks in Fig. 5 cross this regime), or elongated fractured bodies (the transition regime), or reassembled, brecciated spheroids.

A DEFINITION OF COMPARABLE-SIZE BODIES: EXTENSION TO OTHER SIZE RATIOS

All of the above derivations have been carried out for mass ratio of the two colliding bodies, m/M, equalling unity. A complete extension of the present work to other size ratios is beyond the scope of this paper. But we may gain some idea of the m/M ratios which are too large for ordinary cratering by considering what size ratio will produce dispersive fragmentation. As defined in the derivation of equation 5, this is produced by the condition that

total energy brought by projectile m and not lost as heat, etc.	=	enough energy to fragment target M	+	enough energy to disrupt target M.

Thus, from equation 5,

$$k\frac{1}{2}mV_{impact}^2 = S\frac{M}{\rho} + \frac{3}{5}\frac{GM^2}{R}$$

$$\therefore \frac{m}{M} = \frac{2S}{k\rho V_{imp}^2} + \frac{8\pi G\rho}{5kV_{imp}^2}R^2. \qquad (13)$$

This result has been plotted on Fig. 7 for our two types of material. The solid lines give m/M required for dispersive fragmentation, for various specified velocities, for a strong ($S = 4 \times 10^6\ \rho$), dense ($\rho = 3 g/cm^3$) basalt-like material in which the fraction of impact energy available for comminution and ejection of material is $k = 0.5$. The dashed lines give the same results for a weak ($S = 10^4\rho$), lower-density ($\rho = 2$) primitive planetesimal (PP) for which the energy fraction $k = 0.3$.

A number of interesting results can be seen from Fig. 7:

1. In an early swarm of planetesimals with low collision velocities ($V \sim 100$ m/s), relatively large mass ratios ($m/M \gtrsim 10^{-3}$, $r/R \gtrsim 0.1$) were needed to break up our weak (carbonaceous-chondrite-like) PP bodies, and once they reached sizes of 1 km they were harder to break up because of their own gravity.
2. If these bodies reached somewhat more than 10^2 km diameter and, either by metamorphism or melting and resolidification, attained the strength of basalts, then bodies this large would be stable against disruptive fragmentation by any local bodies as long as V remained about 100 m/s. Bodies perturbed from a distant source, attaining higher collision velocities, would be needed. All collisions among local bodies of $m/M \gtrsim 0.2$ and diameter

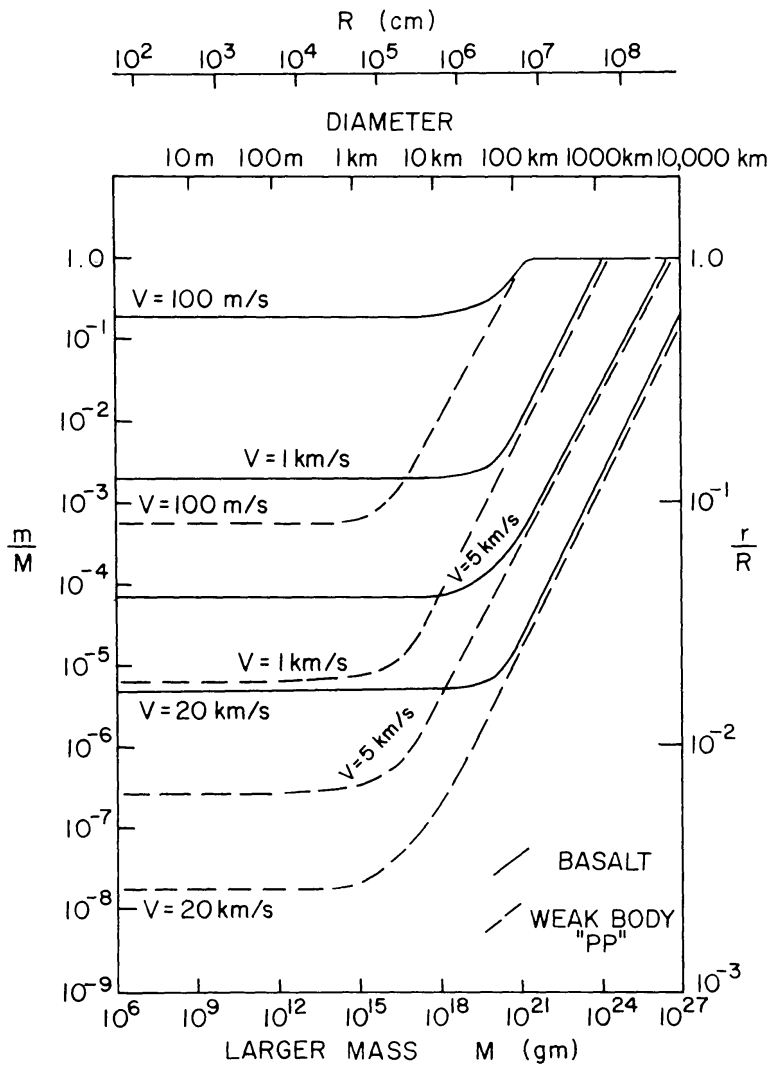

Fig. 7. A definition of "comparable-sized" as used in this paper. The diagram shows the mass and size ratio needed for a smaller body to catastrophically fragment and virtually totally disperse a larger body, as a function of impact velocity (lines labeled V). Extent of reassembly of some fragments is uncertain because of uncertainty in energy partitioning. Solid lines are for pairs of basalt-like bodies; dashed lines are for weakly consolidated material resembling dry soil or weak carbonaceous chondritic primitive planetesimals ("PP"). Above the lines, most of larger mass is dispersed in fragments; below lines, much of the mass reassembles or is not fragmented.

less than about 10^2 km would cause extensive brecciation which would be followed by reaccumulation. (The exact result depends on k, for which fixed values were used here and variable values in Fig. 3, which indicates disruptive fragmentation at about 100 to 1000 km for m/M = 1.)

3. In the asteroid belt today, where $V_{impact} \simeq 5$ km/s, mass ratios as low as $m/M \approx 10^{-6}$ ($r/R \approx 0.006$) could lead to breakup of weakly bonded carbonaceous-chondrite-like bodies up to a few kilometers in size. Mass ratios as low as $m/M \approx 10^{-4}$ ($r/R \approx 0.04$) could lead to breakup of igneous-rock-like

bodies up to ~20 km size. Ceres (D ≃ 1000 km) could be broken by bodies larger than r/R ≈ 0.2, or about 200 km across, of which there are only a few in the whole belt.

4. Jupiter-scattered planetesimals sailing through the inner solar system with impact velocities of the order 20 km/sec could have done great damage. Bodies smaller than a few kilometers could have been disrupted by projectiles with mass ratios of 10^{-8} to 10^{-5} (r/R ≈ 0.002 to 0.01) depending on target strength. Ceres would require a hit by a body only about 100 km across. In support of the theory of moon formation by collisionally induced fission (blow-off of a circumterrestrial cloud of moon-forming debris during a major collision: Hartmann and Davis, 1975; Cameron and Ward, 1976), a Jupiter-scattered planetesimal of 6000 km scale could have disrupted earth, and a somewhat smaller one dislodged a large amount of debris. Safronov's work (1972, p. 134) calls for Jupiter planetesimals up to about 0.005 Jupiter masses, or diameter around 18,000 km. We can expect that many Jupiter-scattered objects passed through the inner solar system (Kaula and Bigeleisen, 1975) and had their effect (Weidenschilling, 1975) through the highest probability fate would have been ejection or Jupiter collision. Actual collisions with growing terrestrial planets would most probably have involved only the smaller jupiter planetesimals (because of the size distribution involved), but these could still be hundreds or thousands of km across—very large bodies in terms of collisional effects on terrestrial planets.

LINES OF EVIDENCE

Five lines of evidence suggest that planetary collisions in the solar system have not been limited to cratering events where one body hits a much larger one.

First, the properties of metallic and ordinary chondrite meteorites indicate that they were formed with burial depths at least of the order 15 to 50 km (Wasson, 1974, p. 185). Pellas and Storzev (1977) conclude that ordinary chondrites were buried at depths about 120 to 200 km. Such dimensions show that these meteorites were not excavated from ordinary cratering events (large lunar and planetary craters are shallower than these figures), but involved breakup of large planetesimals and scattering their intact fragments.

Second, monomict breccias, Wasson's (1974, p. 76) genomict breccias, and especially polymict breccias among meteorites have generally been attributed to collisions, but the current study suggests they may often involve the special case of comparable sized bodies for the following reason. If a large "host" body is simply cratered by smaller meteoroids, the ejecta layers will build up a breccia structure as found on the moon, but the breccia material will be mostly the host rock typical of the region around the sample site. This is especially true if the host body has a regolith, as suggested by Wilkening (1977). Much of the smaller meteoroids will be vaporized if they impact at the high speeds to which they are pumped up by larger bodies in the swarm (cf. Figs. 5 and 6). Due to vaporization

and their inherent relatively small size, they will tend to contribute a small proportion to the resulting breccia. For example, the meteoroid content of lunar soil appears to be only a few percent. On the other hand, colliding comparable sized bodies will often yield a chaotic group of fragments that reassemble into a spheroidal body as discussed in Fig. 2. Most of the volume can thus become brecciated. Many of the fragments originating at a distance from the impact site will not be vaporized or highly metamorphosed; large volumes of incompatible materials will be brought into contact at relatively low speeds during reassembly so as to explain both the abundances and properties of many unusual breccias. Wilkening (1977) notes that foreign meteorites inside other meteorites are common, that "most stony meteorites are breccias" which she regards as mostly products of impacts into regoliths, and that a biasing against reporting of polymict breccias exists since analysts sample "representative" portions. The commonly brecciated classes listed by Wasson (1974, p. 27) total 15% of the falls, about half of which are achondrites or irons, suggesting origin inside substantially large bodies. Modellers of collisions among asteroids should thus give further attention to the fraction of total volume of asteroids that has been "processed" by forming in one parent body, undergoing a collision that fragments the sample, and then reaggregating into a new body brecciated on (say) a centimeter scale. Model asteroid belts with minimal collisional evolution would have low values of this fraction and would preserve many primitive bodies; belts "saturated" by collisional processing could have such fractions near 100%. Observations of the fraction among meteorites or by asteroid belt exploration would constrain asteroid belt models.

A third line of evidence for the importance of collisions of comparable sized bodies is the suspicion that the planet's properties have been affected by collisions with bodies much larger than those forming the craters. Safronov (1972) attributed obliquities to collisions with bodies with diameters as large as 0.3 or 0.4 planetary diameters. Hartmann and Davis (1975) computed sizes of second largest bodies in the planetesimal swarms to be in a similar range; they would have been swept up by collisions. Safronov and Weidenschilling (1979, private communication) have recently considered possible interaction of terrestrial planets and Jupiter-scattered planetesimals of planetary scale. Cameron and Ward (1976) and Hartmann and Davis (1975) suggested that much of the moon's material derived from earth's mantle, being blasted out by a collision with a body ranging from lunar to Martian size.

A fourth line of evidence for the importance of collisions of comparable sized bodies comes from theoretical consideration of initial size distributions of planetesimals. Under today's asteroidal size distribution, a power law mostly derived by fragmentation of smaller bodies, collisions of comparable-sized bodies are much rarer than collisions in which $m/M \ll 1$. But, according to studies of the dust component of the solar nebula (Safronov, 1972; Goldreich and Ward, 1973), the first planetesimals were probably multi-kilometer bodies whose characteristic size was produced by gravitational collapse of dust aggregates. Their size distribution is unknown, but was presumably much more concentrated in a

narrow size range (0.5–50 km?) than the present fragments. Therefore, initially, collisions with m/M > 0.1 would have been more common than today, and interesting products such as unfractured contact binaries, fractured elongated bodies, polymict brecciated spheroids, or co-orbiting pairs of fragments might have been produced. Some of these interesting products may have survived from earlier times until today.

Fifth, a possible example of a body produced by low-speed collision of two comparable-sized bodies may exist in the form of Trojan asteroid 624 Hektor. At $\sim 150 \times 300$ km, it is about twice as long as the other largest Trojans, which are spheroidal. These facts make Hektor difficult to explain by the conventional explanation that elongated bodies are fragments, since one long splinter and a swarm of spheroids seems an unlikely fragment cloud. Hartmann and Cruikshank (1978) suggested that a group of comparable sized bodies grew in the Lagrangian points, and because of the possibility of low-speed approaches of bodies near the Lagrangian points, a pair of such bodies fell together to form an elongated body, Hektor. Comparison of Figs. 3 and 4 indicates that Hektor probably does not fall in the unfractured contact binary field, especially for weak material. However, it does fall near the transition zone for igneous rock materials, particularly if two Trojan asteroids happened to approach with velocities less than 0.1 km/sec. If this were Hektor's origin, it may be a highly fractured elongated body partly preserving the shape of the initial colliding pair. If Hektor is indeed a "fossilized collision in progress," it would shed interesting light on accretion physics and be an exciting target for future exploration. Further applications of these ideas to Hektor and certain other puzzling asteroids are given in my paper currently in press in the *Proceedings* of the Tucson Asteroid Conference (University of Arizona Press, T. Gehrels, Editor).

Acknowledgments—This work was supported by NASA contracts NASW-2909 and NASW-2134. I thank Donald R. Davis, C. R. Chapman, Richard Greenberg, S. J. Weidenschilling, Laurel Wilkening and Mark Cintala for helpful discussions and critiques. This paper is Planetary Science Institute Contribution No. 113.

REFERENCES

Cameron A. G. W. and Ward W. (1976) The origin of the moon (abstract). In *Lunar Science VII*, p. 120–122. The Lunar Science Institute, Houston.

Dunlap J. L. and Gehrels T. (1969) Minor planets III. Light-curves of a Trojan asteroid. *Astron. J.* **74,** 797–801.

Fujiwara A., Kamimoto G., and Tsukamoto A. (1977) Destruction of basaltic bodies by high velocity impact. *Icarus* **31,** 277–284.

Gault D. and Heitowit E. D. (1963) The partition of energy for hypervelocity impact craters formed in rock. *Proc. 6th Hypervelocity Impact Symposium*, vol. 2, p. 219–546. Cleveland, Ohio.

Gault D., Shoemaker E., and Moore H. (1963) Spray ejected from the lunar surface of meteoroid impact. NASA TND-1767, p. 39–41.

Goldreich P. and Ward W. R. (1973) The formation of planetesimals. *Astrophys. J.*, **183,** 1051–1053.

Greenberg R. M. and Hartmann W. K. (1977) Impact strength: A fundamental parameter of collisional evolution (abstract). *Bull. Amer. Astron. Soc.* **9,** 455–462.

Greenberg R., Wacker J., Hartmann W., and Chapman C. (1978) Planetesimals to planets: Numerical simulation of collisional evolution. *Icarus* **35,** 1–26.

Hartmann W. K. (1968) Growth of asteroids and planetesimals by accretion. *Astrophys. J.* **152,** 337–340.

Hartmann W. K. (1977) Large planetesimals in the early solar system. In *Comets, Asteroids, Meteorites* (A. H. Delsemme, ed.), p. 277–281. Univ. Toledo, Toledo.

Hartmann W. K. (1978) Planet formation: Mechanism of early growth. *Icarus* **33,** 50–61.

Hartmann W. K. and Cruikshank D. P. (1978) The nature of Trojan asteroid 624 Hektor. *Icarus* **36,** 353–366.

Hartmann W. K. and Davis D. R. (1975) Satellite-sized planetesimals and lunar origin. *Icarus* **24,** 504–515.

Herndon J. M. and Wilkening L. L. (1978) Conclusions derived from the evidence on accretion in meteorites. In *Protostars and Planets* (T. Gehrels and M. Matthews, eds.), p. 502–510. Univ. Arizona, Tucson.

Kaula W. and Bigeleisen P. (1975) Early scattering by Jupiter and its collision effects in the terrestrial zone, *Icarus* **25,** 18–33.

Levin B. J. (1978) Relative velocities of planetesimals and early accumulation of planets. *Moon and Planets* **19,** 289–296.

O'Keefe J. D. and Ahrens T. J. (1977) Impact-induced partitioning, melting and vaporization on terrestrial planets. *Proc. Lunar Sci. Conf. 8th,* p. 3357–3374.

Öpik E. J. (1965) The cometary origin of meteorites. *Adv. Astron. Astrophys.* **4,** 301–305.

Pellas P. and Storzer D. (1977) On the early thermal history of chondritic asteroids derived by 244–Plutonium fission track thermometry. In *Comets, Asteroids, Meteorites* (A. H. Delsemme, ed.), p. 355–363. Univ. Toledo, Toledo.

Safronov V. S. (1972) *Evolution of Protoplanetary Clouds and Formation of the Earth and Planets.* NASA TTF-677. 71-50049. 206 pp.

Wasson J. (1974) *Meteorites.* Springer Verlag, N.Y. 316 pp.

Weidenschilling S. J. (1975) Mass loss from the region of Mars and the asteroid belt. *Icarus* **26,** 361–366.

Wetherill G. W. (1976) The role of large bodies in the formation of the earth and moon. *Proc. Lunar Sci. Conf. 7th,* p. 3245–3257.

Wilkening L. L. (1977) Meteorites in meteorites: Evidence for mixing among asteroids. In *Comets, Asteroids, Meteorites* (A. H. Delsemme, ed.), p. 389–396. Univ. Toledo, Toledo.